A Neural Map of Auditory Space in the Owl

Abstract. *Auditory units that responded to sound only when it originated from a limited area of space were found in the lateral and anterior portions of the midbrain auditory nucleus of the owl* (Tyto alba). *The areas of space to which these units responded (their receptive fields) were largely independent of the nature and intensity of the sound stimulus. The units were arranged systematically within the midbrain auditory nucleus according to the relative locations of their receptive fields, thus creating a physiological map of auditory space.*

One of the primary functions of the auditory system is to locate sound sources in space. How space is represented in the auditory system, however, is not known. One theory originally put forth by von Békésy (*1*) assumes that sound location is encoded by the relative activation of two populations of neurons, one population sensitive to sound on the right and the other to sound on the left. An alternative theory (*2*) proposes that sound location is encoded as "place" in the nervous system, with individual neurons being sensitive only to restricted portions of auditory space. Neurons which respond best to particular interaural time or intensity disparities have been found at several levels in the auditory pathway (*3*). However, the interaural disparities to which these units are "tuned" are too great and the tuning is too crude to account for the auditory angular acuity of animals measured behaviorally. Consequently, some researchers have rejected the proposition that the auditory system encodes space in terms of receptive fields and neural maps, as in the visual and somatosensory systems, and have opted for the population theory of sound localization (*4*). On the other hand, recent neurophysiological studies, in which sound stimuli were presented in real space, have shown that auditory units can have restricted receptive fields (*5*), a finding that tends to support the place theory of sound localization.

We have begun to explore the influence of sound source location on the response properties of central auditory neurons by using a movable speaker to deliver sound stimuli under free-field conditions. With this approach we have found a region in the owl's midbrain auditory area, nucleus mesencephalicus lateralis dorsalis (MLD), that contains units that respond to sound only when it originates from a small area of auditory space (receptive field) (*6*). Furthermore, these units are systematically arranged within the nucleus according to the azimuth and elevation of their receptive fields so that they form a physiological map of auditory space.

Four barn owls (*Tyto alba*) were used in these experiments. Light anesthesia was maintained with intramuscular injections of Ketamine (4 mg per kilogram of body weight). The experiments were

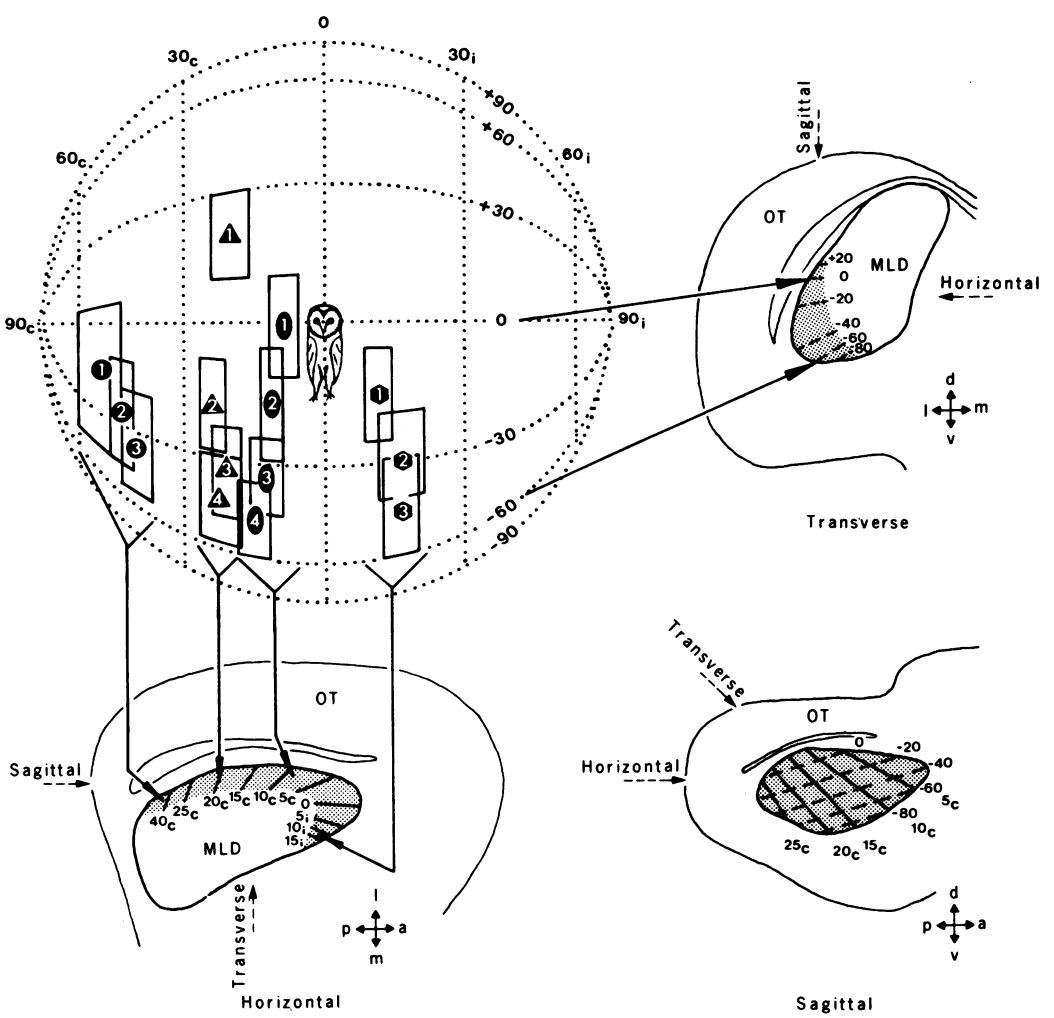

Fig. 1. The representation of auditory space in the MLD, as defined by the centers of unit best areas. In the upper left, the coordinates of auditory space are depicted as a dotted globe surrounding the owl. Projected onto the globe are the best areas (solid-lined rectangles) of 14 units that were recorded in four separate penetrations. The large numbers backed by similar symbols represent units from the same penetration; the numbers themselves signify the order in which the units were encountered and are placed at the centers of their best areas. The penetrations were made with the electrode oriented parallel to the transverse plane at the positions indicated in the horizontal section by the solid arrows. Below and to the right of the globe are illustrated three histological sections through the MLD in the horizontal, transverse, and sagittal planes. The stippled portion of the MLD corresponds to the region that contains only neurons with small receptive fields. Isoazimuth contours, based on best-area centers, are shown as solid lines in the horizontal and sagittal sections; isoelevation contours are represented by dashed lines in the transverse and sagittal sections. On each section dashed arrows indicate the planes of the other two sections. Solid, crossed arrows to the lower right of each section define the orientation of the section: *a*, anterior; *d*, dorsal; *l*, lateral; *m*, medial; *p*, posterior; *v*, ventral. The length of the arrows corresponds to 600 μm. The optic tectum (*OT*) is labeled on each section.

0036-8075/78/0519-0795$00.50/0

conducted in a large anechoic chamber (*7*) specially equipped with a remotely controlled movable speaker (*8*) that could be positioned almost anywhere on a sphere centered at the owl's head (*9*). The owl was oriented so that the intersection of its visual plane and its median plane corresponded to 0° of elevation, 0° azimuth of the speaker (*10*). Sound stimuli included clicks, noise, and tone bursts (*11*). Although the units were tested for sensitivity to visual stimuli (*12*), all auditory tests were conducted with the owl in total darkness.

The auditory units described in this report were recorded from a functionally specialized region of the midbrain that was histologically identified as belonging to the MLD, the avian homolog of the inferior colliculus (*13*). The region forms the lateral and anterior borders of the main, tonotopic portion of the MLD, and extends in a continuous L-shaped strip from the posterolateral to the anteromedial corner of the nucleus (Fig. 1). In all, 182 units were recorded from this region on 47 separate penetrations (*14*).

Units in this region of the MLD shared three salient response properties: (i) they responded only when a sound was located within a well-defined area of space, which was virtually independent of the nature and the intensity of the sound stimulus; (ii) they responded well to clicks, noises, and tone bursts; and (iii) they were tuned to the high-frequency end (5 to 8.7 kHz) of the owl's audible range (*15*).

Auditory receptive fields were plotted in the following manner. After a single unit was isolated, the speaker, while emitting noise bursts, was moved to a location to which the unit responded vigorously. With the speaker at this location the threshold of the unit to noise bursts was determined (*16*). The intensity of the noise bursts was then increased to 10 dB above threshold, and the speaker was moved in azimuth and elevation to positions where the unit just failed to respond. The coordinates of these positions defined the borders of the unit's receptive field (Fig. 2). The same procedure was followed when plotting a field with clicks or tone bursts.

The receptive fields of these MLD units were in the shape of vertically oriented ellipsoids (86 units out of 92) or bands (six units), and ranged in size from 7° to 40° (mean, 25°) in azimuth and from 23° to "unrestricted" in elevation. Both ellipsoidal and band-shaped receptive fields contained a small distinct area within which a sound would induce a maximum response from the unit. This area, which was highly restricted in azimuth and elevation, will be termed the unit's best area. Although a unit's best area could be accurately determined by monitoring spike activity as a test stimulus was moving through its receptive field, more precise measurements of best area were made with the aid of peristimulus time (PST) histograms. The PST histograms were generated through the use of a sound 10 dB above threshold, and were routinely collected at 5° intervals in azimuth and at 10° intervals in elevation, although smaller receptive fields were often sampled at smaller intervals. The extent of a unit's best area was defined by those speaker locations at which the unit first gave a submaximum response (Fig. 2).

Sound intensity had no effect on the location of a unit's best area and had little effect on the size of many receptive fields. When receptive fields plotted with a sound 30 dB above threshold were compared with those plotted with a sound 10 dB above threshold for 63 units, 27 (or 0.4) changed by ±2° or less in azimuth and 14 (or 0.2) changed by ±5° or less in elevation. Twenty-three (or 0.4) expanded in azimuth by 3° to 11° and 13 (or 0.2) contracted by 3° to 18°.

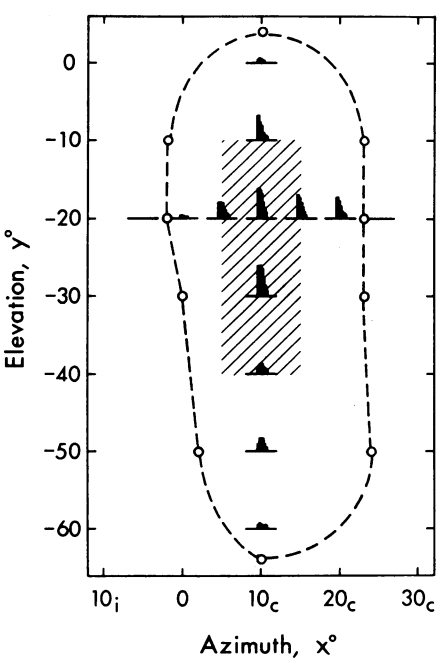

Fig. 2. The receptive field and best area of an MLD unit. Dashed lines mark the borders of the unit's receptive field as projected from actual measurement sites (open circles). The receptive field was plotted using noise bursts 10 dB above threshold. The unit's best area (diagonal lines) was derived from the peristimulus time (PST) histograms shown in the figure. Best-area borders were defined by the first test locations that resulted in a submaximum response. Each PST histogram represents a 200-msec sample of the unit's responses to 16 repetitions of a 100-msec noise burst, presented 10 dB above threshold. The position of each histogram corresponds to the location of the speaker during the accumulation of that histogram. Negative degrees indicate locations in the inferior auditory hemifield; subscript *c*, contralateral and subscript *i*, ipsilateral.

Changing the test stimulus from noise bursts to clicks or tone bursts did not alter a unit's best area, and usually exerted little influence on its receptive field boundaries. Thus, these MLD units sensed a limited area of space that was largely independent of the intensity or the nature of the sound stimulus.

In plotting the receptive fields of these units, it became apparent that the fields of neighboring units were superimposed and that advancement of the electrode resulted in a systematic shift in receptive field location. During a typical penetration, made dorsoventrally and parallel to the transverse plane (*17*), sequential receptive fields would shift continuously in elevation from high to low while moving little in azimuth.

The impression that the units in this region of the MLD were organized according to the location of their receptive fields was confirmed in a series of three experiments in which both the left and right MLD regions were mapped. In these experiments, a total of 19 penetrations traversed the region, sampling units throughout most of its anteroposterior extent. Lesions placed at the sites of the first- and last-mapped units designated the trajectory of each track. The locations of intervening units were reconstructed from their depths with respect to the two lesion sites, as measured by a hydraulic microdrive.

An ordered representation of auditory space was manifest in both the receptive fields and the best areas of these MLD units. However, variations in receptive field size frequently caused irregularities in the spatial transition of the receptive field borders of sequential units. In contrast, unit best areas shifted smoothly and predictably as the electrode advanced. For this reason, and because the center of a unit's best area could be expressed as a single azimuth-elevation term, best-area centers were correlated with unit location to arrive at the detailed map of auditory space representation (Fig. 1).

Sound azimuths were arrayed in the horizontal plane of the MLD, with most of the region devoted to contralateral auditory space. Best-area centers extended from 60° contralateral ($60°_c$), represented in the posterolateral corner, to 15° ipsilateral ($15°_i$), represented in the

anteromedial corner. Azimuths between 20°$_c$ and 0° were disproportionately well represented, but azimuths beyond 30°$_c$ and 10°$_i$ received little representation.

Sound elevation was arranged dorsoventrally in the transverse plane: high best areas were located dorsally; low best areas were located ventrally. Best-area centers ranged in elevation from +20° to −90° with greatest representation given to the area between −10° and −60°.

This map of auditory space is an emergent property of higher-order neurons, distinguishing it from all other sensory maps that are direct projections of the sensory surface. The auditory system must derive its map from the relative patterns of auditory nerve input arriving from the two ears. This requires that (i) there exist unique interaural intensity or time criteria for each area of auditory space, (ii) the auditory input be connected in such a way that each central neuron responds to a slightly different set of criteria corresponding to a slightly different area of space (*18*), and (iii) these neurons be arranged so that the order of their receptive fields conforms to the continuity of auditory space. Because these space-related response properties and functional organization must be specifically generated through neuronal integration by the central nervous system, it seems likely that these neurons in this specialized region of the midbrain are intimately involved in the analysis of spatial aspects of auditory signals.

ERIC I. KNUDSEN
MASAKAZU KONISHI
Beckman Laboratories of Behavioral Biology, California Institute of Technology, Pasadena 91125

References and Notes

1. G. von Békésy, *Experiments in Hearing*, E. G. Wever, Transl. and Ed. (McGraw-Hill, New York, 1960). The theory was later expanded by W. A. van Bergeijk [*J. Acoust. Soc. Am.* **34**, 1431 (1962)].
2. L. A. Jeffress, *J. Comp. Physiol. Psychol.* **41**, 35 (1948).
3. For a review of neurophysiological studies on sound localization, see S. D. Erulkar, *Physiol. Rev.* **52**, 237 (1972).
4. J. L. Hall, *J. Acoust. Soc. Am.* **37**, 814 (1965); F. Flammino and B. M. Clopton, *ibid.* **57**, 692 (1975); A. Starr, *Fed. Proc. Fed. Am. Soc. Exp. Biol.* **33**, 1911 (1974).
5. E. I. Knudsen, M. Konishi, J. D. Pettigrew, *Science* **198**, 1278 (1977); B. Gordon, *Sci. Am.* **227**, 72 (December 1972); F. Morrell, *Nature (London)* **238**, 44 (1972); B. G. Wickelgren, *Science* **173**, 69 (1971); E. I. Evans, in *Ciba Foundation Symposium on Hearing Mechanisms in Vertebrates* (Churchill, London, 1968).
6. By analogy to its connotation in contemporary visual research, the term "receptive field" will refer to the area of space within which a sound stimulus can influence the firing of an auditory neuron.
7. The anechoic chamber measured 3 by 3 by 5 m and was free of standing waves due to reflection for the frequency range used; sound attenuation followed the inverse-square law.
8. The speaker (5 cm) was calibrated with a 2.5-cm condenser microphone (Bruel & Kjaer) placed at the position where the owl would be located. The frequency response of the speaker was flat from 4 to 10 kHz. Variation in sound intensity as a function of speaker location was less than ±2 dB except in a small area directly beneath the owl.
9. The speaker moved in azimuth along a semicircular track 2 cm wide and 2 m in diameter. The track could be rotated to provide changes in speaker elevation. Azimuth and elevation were controlled independently by two stepping motors located outside the chamber. Thus the speaker could be positioned at any point on a sphere of radius 1 m centered at the owl's head, except for a 20° sector blocked by a supporting post for the owl.
10. The highly pigmented pecten oculi in each eye, which is plainly visible ophthalmoscopically, provided a convenient landmark for aligning the owl's head. The visual plane is the horizontal plane containing the projection from each area centralis through the nodal point of the eye to the horizon. In the barn owl the visual plane is located 8° to 10° below the plane containing the projections of the superior limbs of each pecten into space. The owl's visual plane was adjusted by monitoring the projection angle of the superior limbs of the pectens. Medial plane alignment was achieved by positioning the owl so that its pectens projected symmetrically on either side of the 0° azimuth plane.
11. Noise and tone bursts were 100 msec in duration with 2.5-msec rise and decay times and were repeated at a rate of 0.75 to 1 per second. The noise spectrum was 1 to 10 kHz, and the click spectrum predominately 4 to 8 kHz.
12. Units were tested for sensitivity to visual stimuli by sweeping bars and spots of light across a tangent screen temporarily placed 57 cm in front of the owl. The screen was removed during acoustic stimulation. The MLD units were not responsive to visual stimulation.
13. H. J. Karten, *Brain Res.* **6**, 409 (1967).
14. Units were recorded extracellularly with glass-insulated tungsten electrodes. The electrode penetration angle was 45° to the ear canal-beak hinge axis (that is, in the transverse plane) as measured by a protractor.
15. M. Konishi, *Am. Sci.* **61**, 414 (1973).
16. Unit thresholds ranged from −10 to +36 dB sound-pressure level.
17. We have adopted the conventions of H. J. Karten and W. Hodos [*A Stereotaxic Atlas of the Brain of the Pigeon* (Columba livia) (Johns Hopkins Press, Baltimore, 1967)] in defining the planes of section.
18. Attenuation of sound intensity to one ear by earplugging severely altered the receptive fields of these midbrain units.
19. We thank A. J. Hudspeth for critically reviewing the manuscript. This work was supported by an NIH postdoctoral fellowship 1 F32 NS 05529-01 to E.I.K.

6 September 1977; revised 14 December 1977

Intracellular Calcium: Its Movement During Pentylenetetrazole-Induced Bursting Activity

Abstract. *The intracellular calcium concentration in the cytoplasm decreased and the calcium concentration near the cell membrane increased during bursting activity induced by pentylenetetrazole in snail neuron. Incubation in medium containing cobalt chloride or lanthanum chloride did not change this tendency, which suggests that this calcium distribution change is due to the stored calcium in the subcellular structure moving toward the cell membrane.*

The cerebral cortical neuron of the cat shows a characteristic bursting firing pattern on injection of pentylenetetrazole (PTZ) (*1*). Some of the identifiable neurons of *Aplysia* and snails also respond to PTZ application with a characteristic bursting activity or sustained depolarization that strongly resembles the PTZ-induced change in the mammalian cerebral cortical neuron (*2*, *3*). This bursting activity is considered to be of endogenous origin, and these cells generally show negative resistance characteristics in voltage clamping experiments (*4*). Electrophysiological and neurochemical investigations (*5*) have indicated that calcium ion is very important for such bursting activity.

Because of the technical difficulties involved, however, little is known about the intracellular movement of calcium during bursting activity induced by PTZ. The electron probe x-ray microanalyzer (EPXMA) makes possible investigations of intracellular ionic movement in relation to the cellular ultrastructure. We discuss here the calcium and magnesium distribution changes induced by PTZ that are due to intracellular calcium movement.

Identifiable D neurons of the subesophageal ganglion of the Japanese land snail *Euhadra peliomphala* were used. These neurons are more sensitive to PTZ than are other types of neurons (*3*). The ganglia were dissected and divided into two groups, one of which was incubated in snail Ringer solution containing PTZ (5×10^{-2} mole) and the other in normal snail Ringer solution. After 15 minutes of incubation, both groups were dipped into Freon 12 cooled by liquid nitrogen. The Freon 12 was solid except for a small volume, which was melted by a copper block just before the specimens were dipped. The frozen ganglia were freeze-dried in a deep freezer (below −35°C) without passing through a liquid phase. The D neuron was easily picked up from the freeze-dried cluster by use of a fine forceps. Spot analysis of calcium and magnesium was performed.

For computer-controlled mapping of the calcium distribution, the ganglion was prepared so that the D neuron could easily be sectioned later in a freezing chamber. The ganglion was quickly removed, placed on an aluminum holder, and dipped in liquid Freon 12 as described above. A frozen thin section of

0036-8075/78/0519-0797$00.50/0